Magnetic phase separation in artificial *A*-type antiferromagnetic films

Olav Hellwig, Andreas Berger, and Eric E. Fullerton*
San Jose Research Center, Hitachi Global Storage Technologies, San Jose, California 95135, USA
(Received 3 December 2006; published 19 April 2007)

We investigate the domain structures in artificial *A*-type antiferromagnetic (AF) film structures composed of AF-coupled Co/Pt multilayers. By tuning the layer thickness or applying a magnetic field, we observed the coexistence of AF domains and ferromagnetic stripe domains. We find that a ferromagnetic phase exists at AF domain boundaries, causing complex mesoscopic domain patterns with surprising reversibility during minor loop field cycling.

DOI: 10.1103/PhysRevB.75.134416 PACS number(s): 75.60.Ch, 75.70.−i, 75.75.+a

I. INTRODUCTION

An exciting area of materials physics is the increased complexity and emergent behavior arising when building materials from the nanoscale.[1] Local interactions often give rise to higher-level patterns and mesoscopic order driven by competing interactions or multiple phases with similar energies. Complex oxide colossal magnetoresistance (CMR) manganites display such behavior where the interplay of spin, charge, and lattice degrees of freedom triggers spontaneous magnetic phase separation on the nanometer scale.[2] Questions arise whether this phase separation is an intrinsic property of the material or linked to local structural variations and whether this behavior can be controlled and exploited. To explore these rich phenomena it often proves useful to build model structures that mimic more complex materials.[3] In particular, we investigate here the domain structures in artificial *A*-type antiferromagnetic (AF) films,[4,5] a material system that enables us to isolate the complexity arising from the competition between exchange and dipolar energies alone.

Thin-film deposition of magnetic multilayers allows tuning the magnetization, anisotropy, and exchange parameters to design magnetic model materials.[4–7] We recently described Co/Pt-Ru multilayers as a model system for anisotropic *A*-type antiferromagnets.[4,5] Co/Pt multilayers have strong perpendicular magnetic anisotropy for thin Co layers, which yields ferromagnetic (FM) films whose local magnetization is either parallel or antiparallel to the film normal. Layering Co/Pt multilayers separated by Ru interlayers introduces an AF exchange between adjacent $[\mathrm{Co/Pt}]_{X-1}/\mathrm{Co}$ ferromagnetic layer stacks as seen in Fig. 1(a). The resulting heterostructure is a layered anisotropic material with FM intralayer and AF interlayer exchange. These structures mimic the magnetic complexity of a broad range of *A*-type antiferromagnets (e.g., $La_{1.4}Sr_{1.6}Mn_2O_4$),[8–11] but have none of the lattice and electronic state effects that are present in such CMR materials. Thus one hopes to experimentally elucidate the effects arising solely from the magnetic interactions. The results of our study should be applicable more generally to systems with competing interactions, because a Hamiltonian equivalent to the one describing our magnetic multilayer system has also been used to describe the ordering in multiblock achiral liquid crystal molecules with at least one block containing a permanent dipole moment.[12–14]

II. EXPERIMENTAL PROCEDURES

The samples in this study are Pt(20 nm)/$[$[Co(0.4 nm)/Pt(0.7 nm)$]_{X-1}$/Co(0.4 nm)/Ru(0.9 nm)$]_{N-1}$ [Co(0.4 nm)/Pt(0.7 nm)$]_{X-1}$/Co(0.4 nm)/Pt(2 nm)multilayers. In this paper we show primarily results on a uniform $N=12$, $X=7$ sample and a $N=15$, $X=8$ sample in which each of the Co layers form a thickness wedge. All samples were deposited by magnetron sputtering (3 mTorr Ar pressure) onto ambient temperature Si_3N_x coated Si substrates with a 20 nm Pt seed layer and a 2 nm Pt cap for oxidation protection. The multilayer wedge samples have a Co thickness variation of about 10%, while keeping the Pt and Ru thickness constant. Such a slight variation in Co thickness was established by setting the focus of the Co sputtering gun to the outside end of a 5 cm long substrate, which was mounted in radial direction from the center to the edge of the flat circular sample holder. This way it was possible to obtain a wedge structure in the Co layer only, while keeping the substrate holder rotating for otherwise uniform multilayer growth. The average magnetic properties were measured by superconducting quantum interference device and magneto-optical Kerr effect magnetometry. For Co/Pt multilayers, the building blocks of our samples, we find a saturation magnetization of $M_S=700$ emu/cm^3 and a uniaxial out-of-plane anisotropy of $K_U=5\times10^6$ ergs/cm^3. The interfacial AF coupling of the Co/Pt stacks via the Ru interlayers is $J_{\mathrm{AF}}=0.45$ ergs/cm^2. The domain structure was characterized by magnetic force microscope (MFM) using conventional as well as low-moment MFM tips.

III. MAGNETIC PHASES

The results of modeling and experiments of AF-coupled film structures show two magnetic phases depending on the balance of the exchange and the dipolar energy.[4,13–15] Figure 1(b) shows the AF phase with the magnetization of adjacent layers antiparallel, which occurs for strong interlayer coupling. The AF phase can form domains (up-down-up-down vs down-up-down-up) that are characterized by a periodicity λ_{AF}. For the samples described here, λ_{AF} is expected to be large (infinite in the models).[14–16] An experimental realization of this phase is displayed in the magnetic force microscope (MFM) image in Fig. 1(b) showing micron-sized AF domains with strong contrast at their domain boundary.[5]

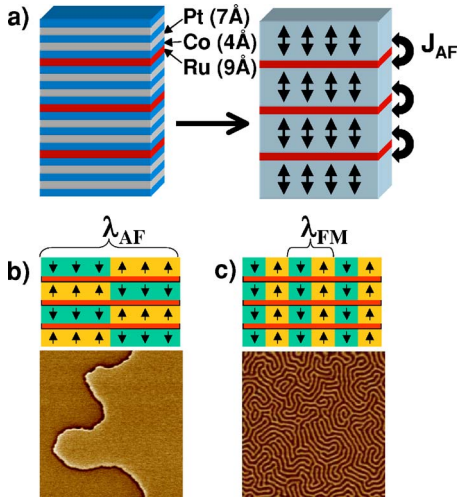

FIG. 1. (Color online) Magnetic phases of the $[[Co(0.4\ nm)/Pt(0.7\ nm)]_{X-1}/Co(0.4\ nm)/Ru(0.9\ nm)]_{N-1}/[Co(0.4\ nm)/Pt(0.7\ nm)]_{X-1}/Co(0.4\ nm)/Pt(2\ nm)$ multilayer model system. (a) Schematic illustration for the case $X=3$ and $N=4$. The Co/Pt stacks can be viewed as uniform FM units with the magnetization pointing either parallel or antiparallel to the film normal. Each ferromagnetic layer stack is AF coupled to its adjacent stacks via Ru interlayers while dipolar fields favor a parallel alignment of the moments in adjacent ferromagnetic layers. (b) AF domain structure of lateral periodicity λ_{AF}. As an example, we show an experimental MFM image $(10\ \mu m)^2$ of a $N=17$, $X=6$ sample after demagnetization showing two AF domains. (c) FM stripe domain structure of lateral periodicity λ_{FM}. As an example, we show an experimental MFM image $(10\ \mu m)^2$ of a $N=18$, $X=9$ sample after demagnetization.

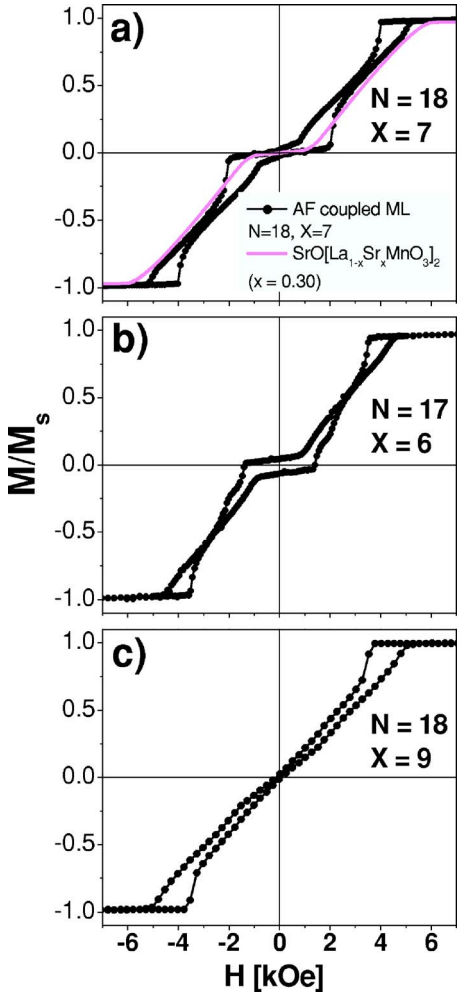

FIG. 2. (Color online) Typical hysteresis loops of the Co/Pt-Ru model system for the exchange dominated phase with (a) $N=18$, $X=7$ and (b) $N=17$, $X=6$, both exhibiting an AF remanent state and the dipolar dominated phase with (c) $N=18$, $X=9$ showing a remanent state of FM stripe domains. In (a) we compare the loop of our Co/Pt-Ru model system with a loop for a $La_{1.4}Sr_{1.6}Mn_2O_4$ crystal from Ref. 9, thus revealing the similar reversal behavior of both systems.

These domains are formed in the system via field cycling.

The second magnetic phase is a FM stripe domain pattern with a periodicity λ_{FM} [Fig. 1(c)]. In this phase the strong dipolar fields prefer a vertically correlated alignment and overcome the AF interlayer exchange. The value of λ_{FM} is determined by the competition between the thin film dipolar energy and the domain wall energy as originally outlined by Kittel[17] for films with perpendicular magnetic anisotropy. This phase is observed experimentally by increasing the number of Co/Pt repeats in each ferromagnetic stack[4] [Fig. 1(c)]. For the specific sample shown here we observe a FM domain period of $\lambda_{FM}=300$ nm which is the same as observed for a Co/Pt multilayer of the same total thickness.

Shown in Fig. 2 are representative magnetic hysteresis loops for two samples with an AF remanent state [Figs. 2(a) and 2(b)] and a FM remanent state [Fig. 2(c)]. Figures 2(a) and 2(c) correspond to the samples shown in Figs. 1(b) and 1(c), respectively. The loop in Fig. 2(c) has a shape characteristic for perpendicular anisotropy magnetic films,[17,18] where the reversal is mediated by stripe domains that couple through the entire thickness of the structure [Fig. 1(b)] as described in Ref. 4. The loops in Figs. 2(a) and 2(b) reflect an *A*-type antiferromagnet with an AF remament state. The loops have three field regions and are typical of AF-coupled films with uniaxial anisotropy.[7] For the low field region the magnetization is relatively constant and near zero for an even N and has a finite value for an odd N corresponding to a single Co/Pt stack. In this region the magnetization is stable in an AF configuration. In high fields (>5 kOe) the Co/Pt stacks are aligned ferromagnetically with the field.

In between we observe the magnetization transitions between the AF and FM states. While in some systems the intermediate region is characterized by a spin-flop phase,[17] the anisotropy of the present system is sufficiently high such that the magnetization remains either parallel or antiparallel to the film normal. This results in the formation of an intermediate state with mixed AF and FM phases. Because of the dipolar interactions the FM regions are correlated through the structure and form stripes (see Sec. IV) in a mechanism similar to that observed for FM films.[17,18] Because of the close connection to the formation of FM stripe domains, the shape of the subloops in Figs. 2(a) and 2(b) are qualitatively similar to the loops shape for the FM sample in Fig. 2(c). A more detailed discussion of the magnetic structure in this

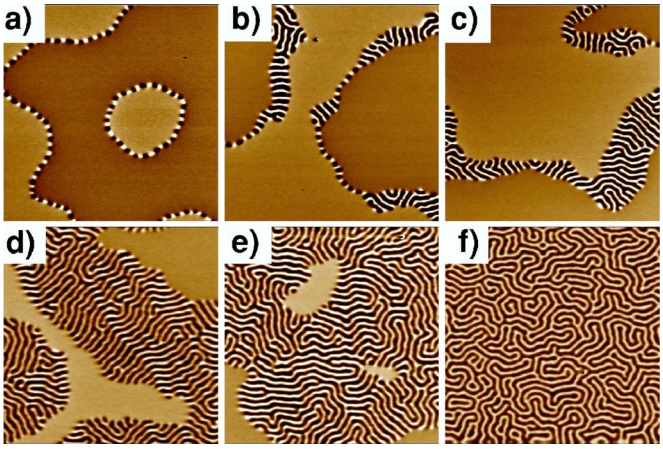

FIG. 3. (Color online) Sequence of MFM images, $(10\ \mu m)^2$ each, showing the two-phase behavior of a multilayer wedge sample with $X=8$ and $N=15$. The Co layers varied continuously from (a) 0.40 nm at the thin end to (f) 0.44 nm at the thick end of the sample and the images were taken in remanence after demagnetization in an oscillating out-of-plane magnetic field by cycling the magnetic field down from 20 kOe to 10 Oe in successive cycles with decreasing amplitude in 0.1% steps. Oppositely oriented AF domains have a slight contrast in the MFM images since the odd number of Co/Pt stacks yields a net magnetization of one stack.

mixed state will be given elsewhere.[19] The same mixed behavior has been observed in single-crystal plates of $La_{1.4}Sr_{1.6}Mn_2O_4$ with the c axis normal to the plate.[9] The similarity of such systems is illustrated in Fig. 2(a) by comparing a hysteresis loop for a $La_{1.4}Sr_{1.6}Mn_2O_4$ crystal from Ref. 9 with one of our Co/Pt-Ru model structures. The loops are nearly identical with the increased hysteresis of the multilayer being the result of the low number of multilayer repeats. The hysteresis is difficult to see in the $La_{1.4}Sr_{1.6}Mn_2O_4$ crystal data, but was clearly determined by a more careful analysis.[9]

IV. TWO PHASE BEHAVIOR

In the remainder of the paper we examine the mixed AF-FM phase behavior of this system, first by tuning the energy continuously between the AF and FM phases and secondly by applying an external magnetic field to the AF domain phase. To follow the transition between the two phases we vary the magnetization of the ferromagnetic layers by depositing multilayer wedge samples, where each of the Co layers varied continuously from 0.40 nm at one end of the sample to 0.44 nm at the other. Close to the AF-FM phase boundary this small change in Co layer thickness is sufficient to change the system from the AF to the FM ground state. Shown in Fig. 3 are six remanent MFM images along the wedge after out-of-plane demagnetization showing the two-phase behavior. For the thinnest Co thickness [Fig. 3(a)] we observe large AF domains with one-dimensional FM stripes at the AF domain boundary. These regions of FM order are stabilized due to the interlayer dipolar fields at the AF domain boundary[5] and have also been observed in other AF-coupled systems.[20] For thinner Co layer thicknesses, the FM order at the AF domain boundary disappears forming the boundary shown in Fig. 1(b).[5] As the Co thickness increases [Figs. 3(b)–3(f)] the one-dimensional stripes broaden and start forming two-dimensional labyrinth stripe domain patterns that are characteristic of the FM phase. These regions of FM stripe domains are exclusively located at the boundary between AF domains as seen most clearly in Figs. 3(b)–3(d). In Fig. 3(e) the FM phase has become dominant with only a few local regions of AF order remaining. In Fig. 3(f) the entire field of view is occupied by the FM stripe phase.

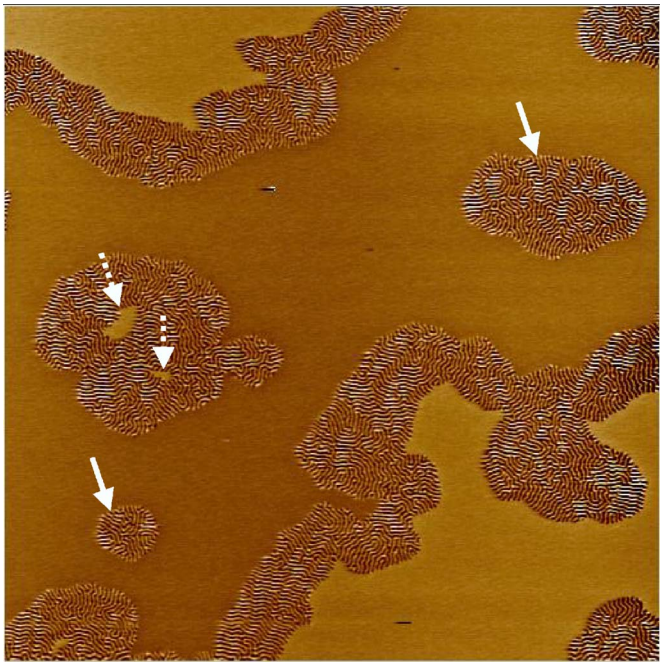

FIG. 4. (Color online) Large scale MFM image, $(50\ \mu m)^2$, from the AF-FM transition range of the wedge sample shown in Fig. 2. The FM stripe domains are found primarily at the boundary between AF domains. The solid arrows highlight FM regions that exist within a single AF domain. The dashed arrows highlight small AF domains isolated at the center of FM regions.

In all of the two-phase coexistence images, we observe that the stripes are oriented normal to the boundary of the AF phase, reflecting the original one-dimensional stripe pattern at low Co thickness [Fig. 3(a)]. The close relation between the presence of the FM phase and the AF phase boundary can be even more convincingly seen in a larger scale image as shown in Fig. 4. Even when the FM phase extends over regions of many microns, the FM order is predominantly at the boundary of AF domains and exhibits a characteristic width. There are examples of isolated FM domain regions within a single AF domain as shown by the solid arrows. We believe that these were formerly smaller AF domains that have been consumed by the FM phase. Such a consumption process is confirmed by the residual AF domains visible in the center of an isolated FM region as highlighted by the dashed arrows. Note that the AF domain remains in the center have opposite contrast to the AF domain surrounding the adjacent FM stripe region.

Figures 3 and 4 highlight the importance of the AF domain boundaries for the observed topography of the two-

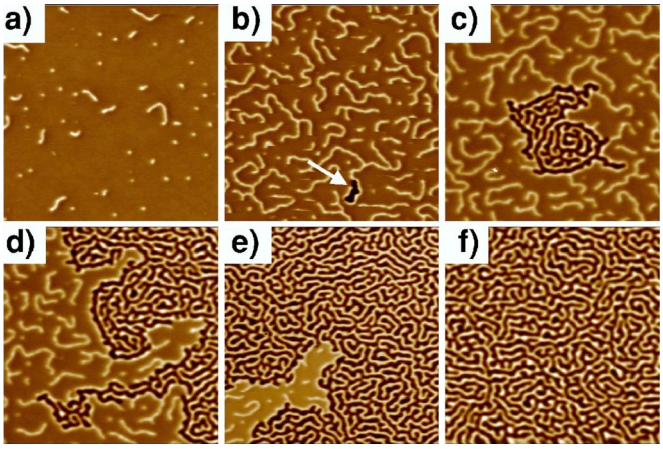

FIG. 5. (Color online) Sequence of MFM images, $(10\ \mu\mathrm{m})^2$ each, showing the two-phase behavior of the multilayer wedge sample from Fig. 2 taken in remanence after prior saturation of the sample in an out-of-plane magnetic field. The arrow in (b) indicates the formation of the first FM stripe domain phase along the wedge.

phase coexistence state. Figure 5 displays six remanent MFM images (of the same wedge sample as shown in Fig. 3) after out-of-plane saturation. Because this particular sample has an odd number of Co/Pt stacks a single AF domain is formed with both surface layers aligned parallel to the saturating field.[7] Consequently there are no AF domains present to facilitate the formation of the FM stripe domain phase as observed in Fig. 3. As the AF phase forms from saturation, there are residual FM regions that persist at remanence showing up as bright lines and dots in Figs. 5(a) and 5(b). As the Co thickness increases, the density of the residual bright FM lines increases until a first dark FM reverse domain nucleates as indicated by the arrow in Fig. 5(b), thus forming the nucleation of the FM stripe phase. As the Co layer thickness increases further we observe extended stripe domain regions that appear to originate from a few nucleation sites.

Not only is the mesoscopic domain order in Fig. 5 quite different from that in Fig. 3, but we also observe a qualitatively different boundary between the FM and AF phase. While after demagnetization FM stripes are oriented perpendicular to the phase boundary we observe a parallel alignment to the boundary in Fig. 5. These differences are observed in the same sample and are caused exclusively by the field history. The boundary between the FM and AF phase in Fig. 5 results from the nucleation process within a uniform AF domain. The FM stripe phase nucleates at the residual FM lines that are present after saturation [Fig. 5(b)]. These lines then provide the boundary between the AF and FM phase, thus resulting in a parallel alignment of the stripe domains with respect to the phase boundary.

Finally we describe the mixed AF and FM order obtained in an external magnetic field being applied to the AF domain phase. The images in Fig. 6 reveal the domain evolution with increasing magnetic field starting from the AF remanent state [Fig. 6(a)] to roughly half the saturation field [Fig. 6(e)] and then back to remanence [Fig. 6(f)]. The remanent state is similar to Fig. 3(a) with AF domains and alternating FM order at the domain boundary. Applying a modest field

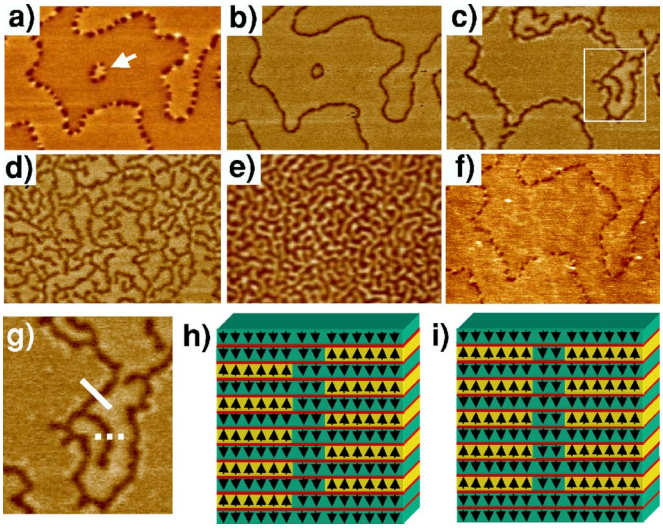

FIG. 6. (Color online) Sequence of MFM images, $\sim(6\ \mu\mathrm{m}\times 4\ \mu\mathrm{m})$, for a sample with $N=12$, $X=7$ and a constant Co thickness of 0.4 nm for different applied field normal to the surface. (a) Remanence with AF domains showing one-dimensional FM stripe domains at the AF domain boundaries. (b) Same image at ~480 Oe applied field, (c) ~960 Oe, (d) ~1150 Oe, and (e) ~1800 Oe. (f) The same image after returning back to remanence after applying fields up to ~2500 Oe. The original domain structure as shown in (a) is preserved with the exception of the small domain highlighted by the arrow in (a). (g) Expanded view of the domain structure in (c) showing the two types of FM regions present in the sample. The solid white line crosses a FM line separating two different AF domains as shown schematically in (h). The dashed white line crosses a FM line separating the same AF domain as shown schematically in (i).

[480 Oe in Fig. 6(b)] stabilizes a uniform FM line at the AF domain boundary by removing the one-dimensional stripe domains. Increasing the field further does not significantly increase the FM linewidth, which is determined by the balance between dipolar and AF exchange energies,[5] but leads to additional FM lines growing out from the domain boundary into the AF phase [Fig. 6(c)]. This growth process continues until the image is filled with a magnetic structure [Fig. 6(e)] consisting of FM lines within two different types of AF domains (up-down-up-down and down-up-down-up). This mixed phase behavior corresponds to the intermediate field regions of Figs. 2(a) and 2(b).

Surprisingly, when the field is removed [Fig. 6(f)] the original AF domain pattern returns [minus the small domain marked by the arrow in Fig. 6(a)]. This microscopic return point memory originates from the nature of the FM lines at the AF domain walls. Shown in Fig. 6(g) is an expanded region of Fig. 6(c), which highlights the two types of FM lines that can be found in the system. The solid white line in Fig. 6(g) crosses a FM region that exists between two different AF phases and is present in zero field [Fig. 6(h)]. However, as the FM domains propagate into the AF phase they have the same AF domain configuration on either side. This is highlighted by the dashed line in Fig. 6(g) and schematically shown in Fig. 6(i) [which is the same spin structure as the FM lines in Fig. 5(a)]. Reversing the field from Fig. 6(e)

causes the FM lines to retract. For any FM line such as shown in Fig. 6(i), the AF phase will be restored as the FM phase retracts. However, the FM lines located at the AF domain boundaries [Fig. 6(h)] are trapped and remain in the system when the field is removed. Since the AF domains have no net moment, neither of them is favored in field cycling and thus the overall AF domain structure remains stable in modest applied fields independent of any local pinning of the domains. This leads naturally to the reversible behavior reflected in Figs. 6(a) and 6(f). This memory effect is only overcome by applying sufficiently high fields that completely remove the AF domain structure.

While such complex domain structures are not expected in exchange-dominated antiferromagnets (e.g., CoO or MnF_2), they do occur in *A*-type and related antiferromagnets.[2,8–11,21,22] Complex mixtures of AF and FM phases are observed both by changing temperature[8,10,11] or field.[9,21,22] In particular, field induced stripe domains have been observed with the morphology of the domains depending on the applied field strength and on defects in the crystal. Our results highlight the role of AF domain boundaries on the topology of the coexistence of AF and FM phases. While such domain structures have not been reported in complex oxides the development of techniques to image AF domains[11,23] should provide opportunities to explore their role. In addition we hope that our experimental findings will motivate domain studies in multiblock achiral liquid crystal molecules and related systems as well as further theoretical study of the two-phase behavior of this model system.

*Present address: Center for Magnetic Recording Research, University of California, San Diego, 9500 Gilman Dr., La Jolla, CA 92093-0401.

[1] R. B. Laughlin, D. Pines, J. Schmalian, B. P. Stojkovic, and P. Wolynes, Proc. Natl. Acad. Sci. U.S.A. **97**, 32 (2000).
[2] E. Degotto, T. Hotta, and A. Moreo, Phys. Rep. **344**, 1 (2001).
[3] R. F. Wang, C. Nisoli, R. S. Freitas, J. Li, W. McConnville, B. J. Cooley, M. S. Lund, N. Samarth, C. Leighton, V. H. Crespi, and P. Schiffer, Nature (London) **439**, 303 (2006).
[4] O. Hellwig, T. L. Kirk, J. B. Kortright, A. Berger, and E. E. Fullerton, Nat. Mater. **2**, 112 (2003).
[5] O. Hellwig, A. Berger, and E. E. Fullerton, Phys. Rev. Lett. **91**, 197203 (2003).
[6] J. B. Kortright, D. D. Awschalom, J. Stohr, S. D. Bader, Y. U. Idzerda, S. S. P. Parkin, I. K. Schuller, and H. C. Siegmann, J. Magn. Magn. Mater. **207**, 7 (1999).
[7] R. W. Wang, D. L. Mills, E. E. Fullerton, J. E. Mattson, and S. D. Bader, Phys. Rev. Lett. **72**, 920 (1994).
[8] T. Fukumura, H. Sugawara, T. Hasegawa, K. Tanaka, H. Sakaki, T. Kimura, and Y. Tokura, Science **282**, 1969 (1999).
[9] U. Welp, A. Berger, D. J. Miller, V. K. Vlasko-Vlasov, K. E. Gray, and J. F. Mitchell, Phys. Rev. Lett. **83**, 4180 (1999).
[10] T. Asaka, T. Kimura, T. Nagai, X. Z. Yu, K. Kimoto, Y. Tokura, and Y. Matsui, Phys. Rev. Lett. **95**, 227204 (2005).
[11] M. Kinoto, T. Kohashi, K. Koike, T. Arima, Y. Kaneko, T. Kimura, and Y. Tokura, Phys. Rev. Lett. **93**, 107201 (2004).
[12] S. I. Stupp, V. LeBonheur, K. Walker, L. Li, K. Huggins, M. Keser, and A. Amstutz, Science **276**, 384 (1997).
[13] M. Sayar, F. J. Solis, M. Olvera de la Cruz, and S. I. Stupp, Macromolecules **33**, 7226 (2000).
[14] M. Sayar, M. Olvera de la Cruz, and S. I. Stupp, Europhys. Lett. **61**, 334 (2003).
[15] A. N. Bogdanov and U. K. Rößler, cond-mat/0606671 (unpublished).
[16] In the theoretical calculations it is generally assumed that there is an even number of layers resulting in no net moment of the AF phase. However, for a small odd number of layers, there remains a significant net moment that may help stabilize a finite λ_{AF}.
[17] C. Kittel, Phys. Rev. **70**, 965 (1946); Rev. Mod. Phys. **21**, 541 (1949).
[18] C. Kooy and U. Enz, Philips Res. Rep. **15**, 7 (1960).
[19] O. Hellwig, A. Berger, J. B. Kortright, and E. E. Fullerton (unpublished).
[20] A. Baruth, L. Yuan, J. D. Burton, K. Janicka, E. Y. Tsymbal, S. H. Liou, and S. Adenwalla, Appl. Phys. Lett. **89**, 202502 (2006).
[21] Ch. Simon, S. Mercone, N. Guiblin, C. Martin, A. Brûlet, and G. André, Phys. Rev. Lett. **89**, 207202 (2002).
[22] Y. Tokunaga, M. Tokunaga, and T. Tamegai, Phys. Rev. B **71**, 012408 (2005).
[23] A. Scholl, J. Stohr, J. Luening, J.-P. Locquet, J. Fompeyrine, J. W. Seo, H. Siegart, F. Nolting, S. Anders, E. E. Fullerton, M. R. Scheinfein, and H. A. Padmore, Science **287**, 1014 (2000).